Conformational and phase transformations of chlorocyclohexane at high pressures by Raman spectroscopy

Zhaohui Dong, Nicholas G. Beilby, Yining Huang, and Yang Song[a)]
Department of Chemistry, The University of Western Ontario, London, Ontario N6A 5B7, Canada

(Received 25 July 2007; accepted 5 December 2007; published online 19 February 2008)

Pressure induced conformational and phase transformations of chlorocyclohexane (CCH) were investigated in a diamond anvil cell by Raman spectroscopy at room temperature. Pure CCH was compressed up to 20 GPa and then decompressed to ambient pressure. The conformational equilibrium was shifted by pressure from equatorial to axial conformers in the fluid phase below 0.7 GPa, consistent with previous observations. Upon further compression, several solid-to-solid phase transitions were identified by the observation of markedly different Raman patterns as well as different pressure dependences of characteristic Raman modes. The possible structures of these phases were analyzed in correlation with previously observed solid phases at low temperatures. Finally, CCH exhibits pressure hysteresis and partial reversibility upon decompression which result in the formation of the phases with different Raman patterns from those obtained upon compression. The difference can be interpreted as conformational contribution as well as the intrinsic plasticity of CCH crystals. © *2008 American Institute of Physics*. [DOI: 10.1063/1.2829408]

I. INTRODUCTION

Conformational and phase transformations as well as unusual chemical reactivities of simple molecular species observed under high pressures have opened new avenues to produce novel structures that are generally inaccessible at ambient conditions.[1] Pressure can significantly alter the interatomic distances and thus the nature of intermolecular interactions, chemical bonding, molecular configurations, crystal structures, and stabilities of solids. With rapid advances in high-pressure technologies,[2] it is feasible to achieve a large compression of lattice, under which condition materials can be easily forced into new physical and chemical configurations. High pressure thus offers enhanced opportunities to discover new phases, either stable or metastable, and to tune exotic properties in a wide range of atomic length scale, substantially greater than those achieved by other thermal and chemical means.[3] Recent studies show that high pressures can essentially lead to physical and chemical changes of molecular solids and modification of their chemical bonds to more delocalized states such as polymeric and metallic phases.[4] Even at moderate pressure regions, e.g., <20 GPa, rich conformational and phase transformations have been observed in several simple molecular systems.[5,6] For instance, we have recently reported a comprehensive analysis of structures of 1,2-dicholoroethane, a simple organic molecule with interesting conformational properties at high pressures using *in situ* Raman spectroscopy.[6]

Similarly, halogen substituted cyclohexane represents another class of simple organic molecules with stereoring structures that exhibit unique conformational behavior. At ambient conditions, it has been well established that the "chair" isomer is thermodynamically more stable than the "boat" isomer by 28 kJ/mol, resulting in the chair isomer being the dominant conformation of cyclohexane.[7] Depending on the spatial orientation of the halogen atom with respect to the ring, for example, chlorocylcohexane (CCH) exhibits two conformations, i.e., axial (a) and equatorial (e), as shown in Fig. 1. The structures of CCH have been extensively studied in all gas, liquid, and solid phases by vibrational spectroscopy.[8–12] In gas, liquid, solution as well as amorphous solid phases, CCH exists as equilibrium mixtures of *a*- and *e*-conformers with higher abundance of the latter, while the crystalline phase consists only *e*-conformer. In addition, the conformational equilibrium was found to change with solvents.[13,14] As either reagent or solvent, CCH has been widely used in many organic reactions, in which the conformational equilibrium plays an important role in determining the product yield as well as reaction kinetics. In addition, the halogenated carbon represents a reaction center to produce stereoisomers as the result of *a*-/*e*-conformation. Therefore, conformational study of this classical ring compound is of fundamental interest.

More intriguingly, CCH exhibits rich temperature and pressure induced polymorphs especially in the solid phase. CCH was found to crystallize into a cubic phase at low temperature and ambient pressure.[15,16] Later on, Diky *et al.*[17] reported a comprehensive study of thermodynamic properties of crystalline CCH. They discovered that crystal I phase,

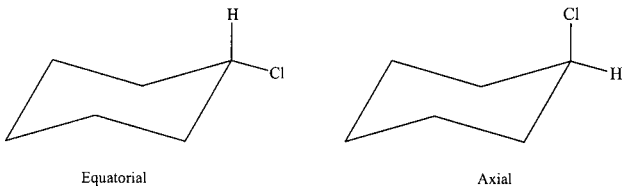

FIG. 1. Equatorial and axial conformers of CCH.

[a)]Author to whom correspondence should be addressed. Electronic mail: yang.song@uwo.ca. Tel.: (519)661-2111 ext. 86310. FAX: (519)661-3022.

which consists of a mixture of *a*- and *e*-conformers, can be formed by cooling down to 229–220 K. When CCH were further cooled to 217 and 206 K, two additional solid-to-solid transitions were identified, resulting in the formation of crystal II and III phases, respectively, both with *e*-conformion exclusively. It has been previously reported that CCH can also form an amorphous phase at 90 K.[10] Independent of temperature tuning, pressure also played a significant role in forming new CCH phases. Using a diamond anvil cell (DAC), Woldbaek reported infrared measurements of CCH at room temperature up to 4 GPa.[10] Detailed analysis indicates that a polycrystalline phase was formed at high pressures and room temperature, which has only *e*-conformer.

Despite the numerous observations of new phases of CCH, no detailed crystallographic structures have been determined due to the lack of high-quality single crystal x-ray data. Furthermore, high pressure can often induce the same phases existing at low temperatures as dictated by the phase diagram. However, for CCH low temperature so far has induced many more new phases than observed at high pressures. Up to date, CCH has only been investigated up to 4 GPa and no further high-pressure Raman measurements have been conducted beyond this pressure. Moreover, the stability of molecules with ring architecture upon extreme compression is of particular interest. An intriguing question is whether the CCH ring will break down as many conjugated ring systems such as benzene[18,19] and furan[20] at certain level of compression. Therefore, it is necessary to extend the previous study to higher pressures to fully understand the structures and properties of CCH. In this study, we report the *in situ* Raman measurements of CCH at high pressures up to 20 GPa, far beyond those previously achieved. Our objective is to explore the unknown pressure domain which may provide important insight in the interpretation of general behaviors of simple organic molecular solids under extreme conditions. We observed rich pressure behavior of CCH and examined the reversibility of phase transformations by both compression and decompression. These new observations contribute to the understanding of high-pressure structures, stability, as well as thermodynamic properties of CCH.

II. EXPERIMENTAL

Pure CCH (99%) was purchased from Aldrich and used without further purification. In the low pressure region, a lever-arm type DAC (purchased from High Pressure Diamond Optics Inc.) equipped with type I diamonds with culet size of 650 μm was used, which allows the accurate control and fine increments of the pressure up to 4 GPa. Stainless steel gaskets were predrilled with a hole of 250 μm as sample chamber. In the high-pressure region, another symmetric piston-cylinder type DAC equipped with 400 μm culet diamond anvils was used to achieve pressures up to 20 GPa. The samples were loaded at room temperature as liquid with nominal pressure slightly above ambient. Then the cell is carefully pressurized with small steps and allowed to stabilize for a few minutes after each pressure change before Raman spectra were taken. A few ruby (Cr^{3+} doped α-Al_2O_3) chips as the pressure calibrant were carefully placed inside the gasket sample chamber before the sample was loaded. The pressure was determined from the well known pressure shift of the R_1 ruby fluorescence line with an accuracy of ± 0.05 GPa under quasihydrostatic conditions.[21] For the entire pressure region, ruby fluorescence spectra obtained on different ruby chips across the sample chamber indicate no significant pressure gradient. Especially at the lower pressure region (e.g., <10 GPa), the ruby spectral profiles suggest no obvious nonhydrostatic effects. Therefore, no pressure transmission media was used.

A commercial Renishaw Ramam spectrometer (model 2000) was used for pressure determination and Raman measurements. This model is a compact laser Raman microprobe capable of both spectroscopy and imaging. A HeNe laser with wavelength of 632.8 nm was used as the excitation source with an average power of several miliwatts on the sample. A Leica microscope with objective lenses of multiple magnifications together with other Raman optics enables measurements with backscattering geometry. An edge filter is installed to remove the Rayleigh and anti-Stokes lines enabling a measurable spectral range above 120 cm^{-1}. The spectrometer is equipped with an imaging spectrograph and a sensitive thermoelectronically cooled CCD detector allowing a spectral resolution of 1 cm^{-1}. Frequency calibration of the Raman spectrum was realized using silicon and diamond standards achieving an accuracy of ± 0.5 cm^{-1}. Due to the strong T_{2g} mode of type I diamond Raman signal at 1334 cm^{-1}, the spectra were collected in the ranges of 120–1300 and 2400–3300 cm^{-1}. These frequency ranges covered almost all the Raman active modes of CCH that are playing important roles in characterizing the conformational and phase transformations. Pressure effects on CCH were examined both in the compression and decompression directions. Experiments were conducted up to 20 GPa and reproduced several times. All measurements were conducted at room temperature.

III. RESULTS

Raman spectrum of liquid CCH was collected at ambient pressure and room temperature as a starting point, which is depicted in Fig. 2(a). The assignments are labeled above each mode and also listed in Table I in comparison with previous measurements under different conditions. Both axial and equatorial conformers have C_s symmetry which thus results in 48 fundamentals (of 27 A' and 21 A'' symmetries), all of which are both Raman and IR active. We note that some vibrations, such as ν_{24}, ν_{23}, ν_{22}, and ν_{21} are observed in both *a*- and *e*-conformations but with drastically different frequencies. The difference is indicated in parentheses in Table I and implied in the context. As can be seen, almost all 48 Raman modes are observed, and their frequencies are consistent with those previously reported under similar conditions. In the liquid phase, CCH exists as a mixture of *a*- and *e*-conformers with the latter being the dominant conformation.

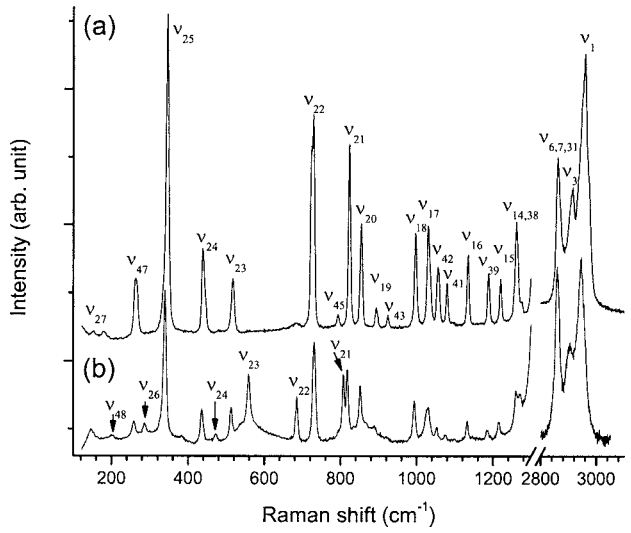

FIG. 2. Raman spectra of CCH collected at (a) ambient pressure in comparison with that (b) collected upon slight compression (0.03 GPa). CCH exists as a mixture of axial and equatorial conformers with the latter dominant at condition (a) and thus the assignment labeled above each Raman modes refers to equatorial conformation. Axial and equatorial conformers share majority of common Raman modes and thus only those exclusively associated with axial conformer are labeled in spectrum (b). The spectral region of 1300–2800 cm^{-1} is omitted due to the strong T_{2g} Raman mode of diamond anvil and that only a few insignificant Raman modes occur in that region.

A. Raman spectra of CCH on compression

When CCH is slightly compressed from ambient pressure to 0.03 GPa, dramatic changes of the Raman spectrum are observed as shown in Fig. 2(b). New bands at 201, 286, 560, 682, and 809 cm^{-1} with significant intensities are attributed to the respective ν_{48}, ν_{26}, ν_{24}, ν_{23}, ν_{22}, and ν_{21} modes exclusively associated with *a*-conformation. Simultaneously, peaks at 262, 438, 517, and 729 cm^{-1} due to the respective ν_{47}, ν_{24}, ν_{23}, and ν_{22} modes are depleted significantly, indicating these modes are mainly associated with *e*-conformation. All other modes shift to low frequencies systematically by a few wave numbers compared to the ambient pressure measurement. The two conformers of CCH have the same symmetry with the only difference in the orientation of chlorine atom. Thus, the shifts can be attributed to the conformational difference between the same modes involved rather than pressure effect, since the pressure difference of 0.03 GPa is negligible. All these observations indicate that the conformational equilibrium has shifted from equatorial to axial significantly. Among these modes, ν_{26}, ν_{24}, ν_{23}, and ν_{21} modes (286, 473, 560, and 729 cm^{-1}), and particularly ν_{22} mode (680 cm^{-1}), which are associated with carbon-chlorine stretching, can be used to monitor the abundance of axial conformation quantitatively. When pressure is increased to 0.5 GPa, for instance, the intensity of all these characteristic Raman modes increased significantly, indicating that the equilibrium is further shifted to axial by pressure.

Instead of continuous enhancement, however, the above mentioned characteristic modes of axial conformation suddenly disappeared completely when pressure is increased to around 0.7 GPa (Fig. 3). In addition, the intensities of the Raman modes of the lowest two frequencies (ν_{27} and ν_{48}) are significantly depleted. In contrast, the modes associated with equatorial conformer, such as ν_{45}, ν_{19}, and ν_{43} at respective 789, 891, and 923 cm^{-1} are markedly enhanced. The observation of such a discontinuity indicates a complete transformation from a mixture of two conformers with axial being dominant to pure equatorial conformation, concurrent to the phase transition from liquid to solid, which is further confirmed by visual inspection under the optical microscope. This is consistent with previous report that solid CCH is composed of equatorial conformers only.[8–12]

The next transformation is observed when CCH is compressed to 2.4 GPa. The most prominent evidence is the observation of the splitting of the ν_{21} mode at 729 cm^{-1}, which appears with a shoulder and then evolves into a well resolved doublet at 4.8 GPa. Furthermore, the Raman modes associated with C–H stretching in the high frequencies (e.g., 2800–3000 cm^{-1}) are significantly weakened by compression to 2.4 GPa, which confirmed the phase transition around this pressure.

When pressure is elevated to 4.8 GPa, modifications of the Raman profile with new features are observed in addition to the pressure induced frequency shift of all Raman modes. Specifically, a new peak appeared in low frequency region at 142 cm^{-1} which is likely associated with lattice vibrations. Another interesting observation is that in addition to the continuing enhancement of ν_{45}, ν_{19}, and ν_{43} modes, the relative intensities of the ν_{21} and ν_{20} modes exhibit a switchover at 4.8 GPa, below which ν_{20} dominates but above which ν_{21} is much stronger. In addition to the splittings of the ν_{22} mode, many other modes also experienced significant splittings, such as ν_{20}, ν_{17}, and ν_{42} modes. The high frequency C–H stretching modes remain weak. All these observations suggest another transition around 4.8 GPa.

As the CCH is compressed to 10.1 GPa, all Raman bands become significantly broader with low frequency modes greatly depleted. Simultaneously, many of the doublet start to merge, such as the ν_{22}, ν_{20}, ν_{17}, and ν_{42} modes. This trend is continuing with increasing pressure up to about 20 GPa, the highest pressure of the present study, where the spectrum displays a profile with broad bands with two strongest modes (ν_{25} and ν_{22}), which are also the strongest observed at low pressures.

B. Raman spectra of CCH on decompression

The reversibility of pressure effect on molecular structures provides important information on transformation mechanisms. Therefore, upon compression of CCH to the highest pressure of 20 GPa, we conducted Raman measurements on decompression all the way down to the ambient pressure. The spectra are depicted in Fig. 4. In general, the change of Raman profile is very gradual with decompression. Not until 10.4 GPa, did all the characteristic modes start to be observed. Compared to the compression data at 10.1 GPa (Fig. 3), a striking difference is the appearance of a new peak at 595 cm^{-1}. In addition, the ν_{22} mode (at 743 cm^{-1}) which appears as a doublet during compression between 2.4 and 10.1 GPa seems to remain a singlet at all pressures during decompression. Instead of being a branch of the doublet, the

TABLE I. Assignment of vibrational frequencies of observed Raman modes of chlorocyclohexane at near ambient pressure and room temperature. Because of strong Raman signal from the diamond anvils, the nearby modes (around 1334 cm^{-1}) were not observed or tabulated.

This work (cm^{-1})		Reference (cm^{-1})[a]				Description
0 GPa	0.03 GPa	Liquid	Crystal (90 K)	Calculated	Assignment[b]	
151/181	145	145	150/167	154	$\nu_{27}A'$	C–Cl bend
	201	200		182	$(\nu_{48}A'')$	Ring bend
262	258	260	260	263	$\nu_{47}A''$	
	286	287		290	$(\nu_{26}A')$	
347	339	341	342	342	$\nu_{25}A'$	
438	438	437	436	428	$\nu_{24}A'$	
	473	473		482	$(\nu_{24}A')$	
517	513	513	513	508	$\nu_{23}A'$	
	560	560		552	$(\nu_{23}A')$	
	682	687		680	$(\nu_{22}A')$	C–Cl stretch
729	729	732	726	733	$\nu_{22}A'$	
794		790	791	787	$\nu_{45}A''$	CH_2 rock
	809	809		806	$(\nu_{21}A')$	
823	818	819	819	819	$\nu_{21}A'$	Ring stretch
855	852	853	851	839	$\nu_{20}A'$	
895	890	890	890	892	$\nu_{19}A'$	
921	919	922	922	928	$\nu_{43}A'$	CH_2 rock
997	992	995	996	992	$\nu_{18}A'$	Ring stretch
1030	1030	1030	1028	1028	$\nu_{17}A'$	
1058	1050	1052	1053	1051	$\nu_{42}A''$	CH_2 twist and wag, CH def
1080	1075	1075	1076	1083	$\nu_{41}A''$	
1134	1133	1132	1133	1121	$\nu_{16}A'$	
1188	1185	1186	1186	1182	$\nu_{39}A''$	
1220	1215	1216	1218	1221	$\nu_{15}A'$	
1263	1262	1261	1261	1251	$\nu_{14}A'$	
				1245	$\nu_{38}A''$	
2864	2859	2861	2855	2853	ν_6A'	CH_2 and CH stretch
				2852	ν_7A'	
				2851	$\nu_{31}A''$	
2915	2903	2908	2907	2914	ν_3A'	
	2944	2946	2943	2922	ν_2A'	
2958			2957	2956	ν_1A'	

[a]Reference 10.
[b]The Raman modes exclusively associated with axial conformation are denoted in parentheses. Other assignments apply to both equatorial and axial conformers.

shoulder peak preceding the ν_{22} mode at 10.4 GPa apparently evolves as an independent mode as pressure is further released and is observed all the way down to 2.5 GPa. Furthermore, the relative intensities of ν_{21} and ν_{20} modes are drastically different between compression and decompression. During compression, the ν_{21} mode remains dominant while the ν_{20} mode is always stronger or equally strong as ν_{21} on decompressions until 2.5 GPa. In addition, many doublet modes observed upon compression, such as ν_{20}, ν_{17}, and ν_{42} modes, appear as a broad singlet during decompression. For example, the most evident comparison can be made between the decompression spectrum at 5.9 GPa (Fig. 4) with the compression spectrum at 5.8 GPa (Fig. 3). In general, the decompression spectra are broader than the compression spectra at corresponding similar pressures. Decompression spectra do not exhibit clear low frequency lattice modes until 2.5 GPa. All these observations indicate that the structural transformations have certain hysteresis upon decompression and are thus not completely reversible at the high-pressure region (>2.5 GPa).

When pressure is released to 2.5 GPa, the Raman spectrum is more or less similar to the one at 2.4 GPa upon compression, except for slightly different intensities as well as the above mentioned new modes, which remains the most distinctive difference. Another major difference is observed in the high frequency C–H stretching region where the decompression spectrum showed three clearly resolved bands, in contrast to a broad profile in the compression spectrum.

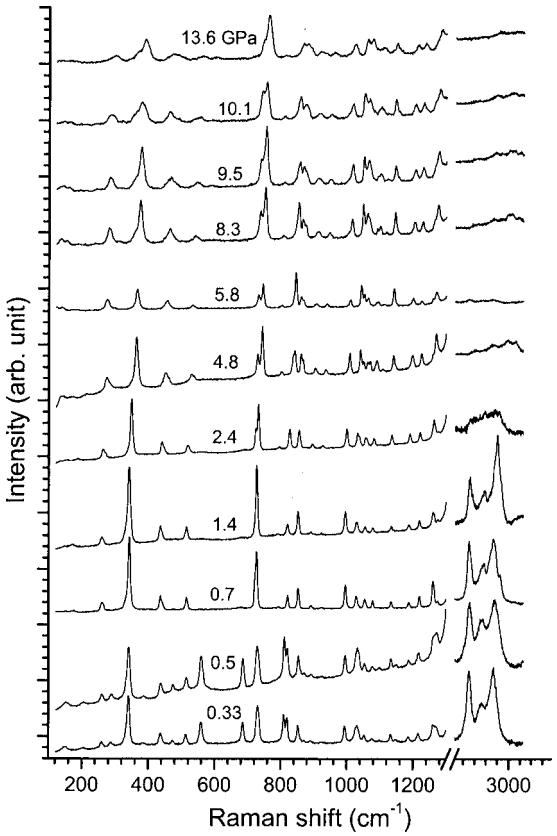

FIG. 3. Selective Raman spectra of CCH on compression in the pressure region of 0–14 GPa in the spectral ranges of 120–1300 and 2800–3200 cm^{-1}. The relative intensities are normalized and thus are directly comparable. The pressures in gigapascals are labeled for each spectrum. The spectra are offset vertically for clarity.

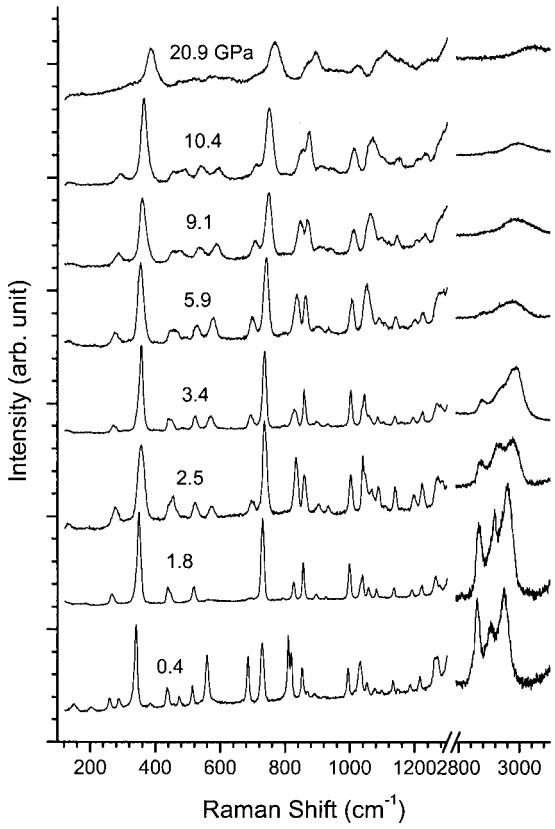

FIG. 4. Selective Raman of CCH on decompression from around 20 GPa all the way down to ambient pressure. The relative intensities are normalized and thus are directly comparable. The pressures in gigapascals are labeled for each spectrum. The spectra are offset vertically for clarity.

When pressure is further released to 1.8 GPa, the Raman pattern exhibits exactly the same features as the one at 1.4 GPa during compression, indicating that the transformation at this pressure is completely reversible. Further releasing the pressure to 0.4 GPa results in the Raman pattern exactly the same as the one at 0.5 GPa during compression, which is attributed to the mixtures of axial and equatorial conformations of CCH. Again, the transformation here is reversible.

C. Pressure effect on Raman modes of CCH

Pressure dependence of selected Raman modes of CCH on compression is depicted in Fig. 5 in the frequency region below 1300 cm^{-1}. Since the C–H stretching modes at 2800–3000 cm^{-1} are observed clearly only below 2.4 GPa, they were not included in the analysis here. The pressure dependences ($d\nu/dP$) of selected Raman modes are listed in Table II as well. In general, all Raman modes exhibit pressure induced blue shifts (with only a few exceptions in the low pressure region as discussed below), consistent with that the bonds become stiffened by pressure. However, at different pressure regions, the shift rates are different, providing evidence for phase transformations.

The first phase transition corresponding to a fluid to solid transition occurs at about 0.7 GPa as indicated by the first vertical dashed line in Fig. 5. Below this pressure, the CCH is composed of a mixture of *a*- and *e*-conformers. Most Raman modes associated with *a*-conformer, such as the ν_{26}, ν_{24}, and ν_{23} (ring bending) modes at respective frequencies of 286, 473, and 560 cm^{-1} as well as the ν_{22} (CH rocking) mode at 729 cm^{-1}, are fairly insensitive to pressure (i.e., $d\nu/dP \approx 0$). Other modes, such as ν_{48} and ν_{21} at 201 and 809 cm^{-1}, shift with pressure more significantly. On the other hand, all modes associated with *e*-conformer generally exhibit large, linear, and positive pressure dependences except for the ν_{22} and ν_{19} modes, which have negative $d\nu/dP$ values (−1.4 and −0.4 cm^{-1}/GPa, respectively). At 0.7 GPa, all the characteristic *a*-conformer modes (ν_{48}, ν_{26}, ν_{24}, ν_{23}, and ν_{22}) disappeared abruptly, indicating that the solid phase is exclusively *e*-conformer.

The major evidence for the second phase transition around 2.4 GPa is the observation of the splittings of ν_{22} C–Cl stretching mode at 729 cm^{-1} into a doublet. Above 2.4 GPa, the two branches of the doublet (labeled as ν_{22} and ν'_{22}) exhibit different pressure dependences with 4.5 versus 2.1 cm^{-1}/GPa. All other modes have similar pressure dependences across the transition boundary around 2 GPa with two exceptions: (1) the ν_{45} mode has a negative $d\nu/dP$ below 2.4 GPa, which becomes positive above 2.4 GPa; and (2) the ν_{17} mode has a much larger pressure dependence (8.0 cm^{-1}/GPa) below 2.4 GPa than above (1.7 cm^{-1}/GPa). These observations, together with the weakening and disappearance of C–H stretch modes at 2859, 2903, and 2944 cm^{-1} (not shown in Fig. 5), clearly confirm the phase transition.

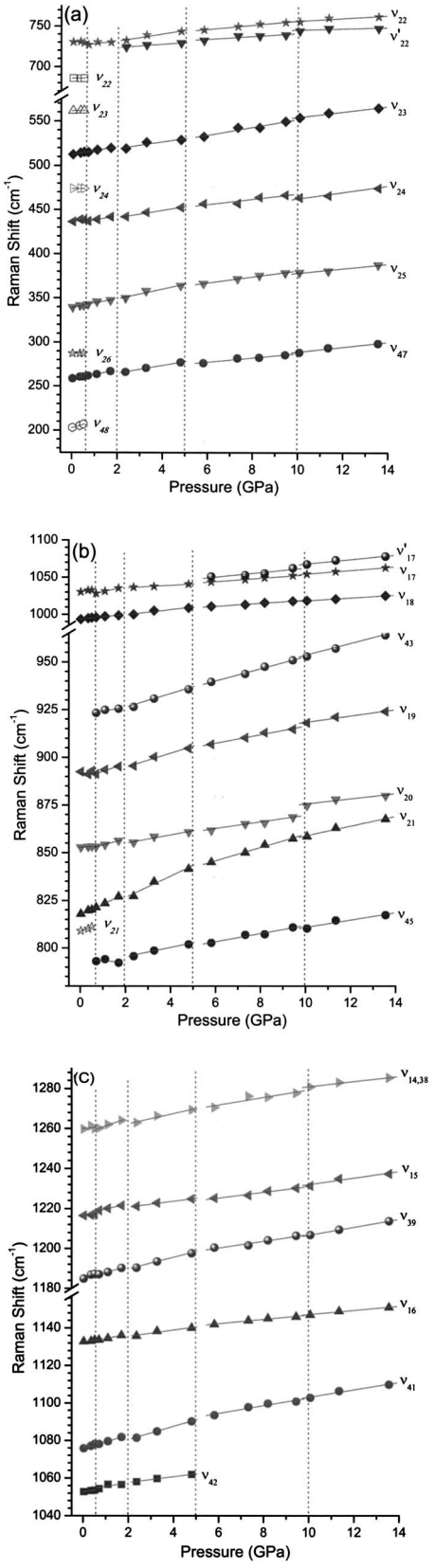

FIG. 5. Pressure dependence of Raman shift of CCH on compression in (a) the ring bending and C–Cl stretching region (180–750 cm^{-1}); (b) the ring stretching and CH_2 rocking region (790–1100 cm^{-1}); and (c) the CH_2 twisting and wagging as well as the CH deformation region (1050–1280 cm^{-1}). Different symbols denote Raman modes with different origins. Open and closed symbols denote axial and equatorial conformers of CCH, respectively. The solid lines crossing the symbols are based on linear fit. The vertical dashed lines denote the proposed phase boundaries.

For the phase between 5 and 10 GPa, all Raman modes exhibit smooth pressure shifts and similar shift rates as those for the phase between 2 and 5 GPa. As described previously, however, several modes exhibit significant splittlings in this pressure region, such as ν_{22}, ν_{20}, ν_{17}, and ν_{42} modes, although not all of them are plotted in Fig. 5 for clarity purpose. The most distinctive discontinuity is the abrupt disappearance of ν_{42} modes above 5 GPa. These features label the second solid-to-solid transition at this pressure. The last transition at around 10 GPa is characterized with much less prominent changes of pressure dependences than the previous several transition pressures.

IV. DISCUSSION

Quantitative analysis of conformational equilibrium of CCH at low pressure region has been addressed by both IR spectroscopy in a solution[13] and Raman spectroscopy as a pure substance.[11] By monitoring the relative intensities of the respective ν_{22} modes at 682 and 729 cm^{-1} associated with axial and equatorial conformations, the equilibrium constant K and volume difference ΔV between the two conformers at certain pressures can be related by

$$\Delta V = -RT\left(\frac{\partial \ln K}{\partial P}\right)_T \tag{1}$$

where T is the temperature, R the gas constant, and K can be evaluated by the ratio of the integrated intensities of the two modes.[6,11] The volume difference ΔV between the two conforms was determined to be −2.33 cm^3 mol^{-1} by Gardiner, in contrast to that by Christian who reported −1.87 cm^3 mol^{-1}, but the latter was obtained in carbon disulphide solution.[13] Based on our measurement, we determine the ΔV to be −2.2 cm^3 mol^{-1} for pure CCH, closer to that by Gardiner as expected.

Studies of volume difference between conformers have been carried out in several other systems under various pressures, temperatures, as well as solvent conditions. For instance, Gardiner conducted a similar study on bromocyclohexane and reported a similar ΔV value (−2.2 cm^3 mol^{-1}) between the axial and equatorial conformers.[22] For different molecular systems, the relative magnitude of ΔV values derived under different conditions (e.g., as a pure substance versus in solutions) is strongly contrasting. In our previous high-pressure Raman study of 1,2-dichloroethane, we found the ΔV that value between *trans* and *gauche* conformers of pure substance (0.58 cm^3 mol^{-1}) is much smaller than in solutions (1.8–4.5 cm^3 mol^{-1}),[6] in contrast to those for CCH where ΔV value in solution is smaller. It has been known that several factors, such as orientation of the substituent, intermolecular interactions, as well as relative packing efficiency, strongly affect the volume difference between the two conformations.[22] Therefore, the combination of different conditions (pressure, temperature and use of solvent with different polarities) will contribute differently to the ΔV values between two conformers with very different structures. Apparently, the larger volume difference between two conformers observed in pure CCH indicates that one or more of the three factor are manifested more than in solutions.

TABLE II. Pressure dependence of vibrational frequencies of major Raman modes for CCH at room temperature. All the Raman modes monitored are associated with the equatorial conformation. The modes for CH_2 and CH stretching region (2800–3000 cm^{-1}) are not tabulated since they are observed only in the low pressure region (<2.4 GPa).

Raman mode[a]	Peak origin (cm^{-1})	$(d\nu/dP)_\tau$(cm^{-1}/GPa)				
		0–0.7 GPa	0.7–2 GPa	2–5 GPa	5–10 GPa	>10 GPa
ν_{47}	262	4.4	5.2	4.5	2.5	2.8
ν_{25}	347	4.8	4.3	5.6	3.4	2.6
ν_{24}	438	5.0	4.9	4.2	3.1	3.7
ν_{23}	517	5.5	4.7	3.8	4.5	3.1
ν'_{22}	⋯	⋯	⋯	2.1	1.8	0.8
ν_{22}	729	–1.4	2.8	4.5	2.6	1.7
ν_{45}	794	⋯	–1.0	2.4	2.2	1.9
ν_{21}	823	4.5	5.8	5.6	3.5	2.6
ν_{20}	855	1.0	3.2	2.2	1.7	1.3
ν_{19}	895	–0.4	3.9	3.7	2.2	1.6
ν_{43}	921	⋯	2.1	3.6	3.2	3.0
ν_{18}	997	4.0	2.6	3.5	2.0	1.9
ν_{17}	1030	5.1	8.0	1.7	2.3	2.4
ν'_{17}	⋯	⋯	⋯	⋯	3.0	2.9
ν_{42}	1058	1.7	2.0	1.5	⋯	⋯
ν_{41}	1080	4.6	3.7	3.5	2.1	2.0
ν_{16}	1134	1.5	2.4	1.7	1.1	1.1
ν_{39}	1188	5.0	3.3	2.9	1.7	2.0
ν_{15}	1220	1.2	2.5	1.5	1.4	1.6
$\nu_{14,38}$	1263	1.1	4.0	2.5	1.8	1.3

[a]The assignments of the Raman modes are consistent with Table I except for ν'_{22} and ν'_{17}, which are new modes observed as a result of splitting of the ν_{22} and ν_{17} modes, respectively.

Based on the high-pressure Raman measurements, the first solid phase exists between 0.7 and 2.4 GPa. This solid phase consists of equatorial conformer exclusively, consistent with previous studies conducted at room temperature and high pressure where CCH forms a polycrystalline phase when compressed up to 4 GPa from liquid.[10] It is well known that high pressure and low temperature generally result in the formation of phases with the same crystalline structure. In an IR study of CCH at ambient pressure and low temperatures,[17] however, the first crystalline phase (crystal I) which was formed by cooling the liquid to 224 K consists of a mixture of axial and equatorial conformers instead of pure *e*-conformer observed as the first solid phase here. Crystal I phase remains stable between 220 and 229 K. Therefore, our observation of systematic absence of characteristic Raman modes associated with axial conformer indicates that the first solid phase of CCH induced by pressure is different from that induced by temperature and is possibly a polycrystalline phase as reported by Klaeboe and Woldbaek.[9,10] The sharp Raman profile characterized by very narrow bandwidth (e.g., ν_{25} and ν_{22} modes) together with the complete phase transformation is consistent with the formation of a crystalline structure under a near perfect hydrostatic condition. However, the detailed structure of this polycrystalline phase has not been characterized by x-ray diffraction to date.

The next solid-to-solid phase transition is observed at 2.4 GPa, which is evidenced by the splitting of ν_{22} mode at 729 cm^{-1} and the disappearance of C–H stretching modes at high frequencies. The splittings and disappearance of certain modes can be interpreted as enhanced intermolecular interactions within the same crystal structure. First of all, the splitting indicates that there are at least two molecules per unit cell in this phase. Pressure induced splitting of Raman modes have been observed in many other molecular solids.[5,6] In addition, dramatic change of the Raman intensity of C–H stretching mode suggests that solid CCH is highly compressible in this pressure region as characterized by much shorter intermolecular distance and smaller molecular volume. As a result, the polarizability of symmetrical stretching and other vibrations associated with a significant change of volume is reduced by the application of pressure and thus their intensities are markedly lowered.[11]

The phase change above 4.8 GPa can be consider as a continuation of enhanced intermolecular interaction as a result of compression. The lack of sharp changes of Raman profiles indicates the transition may involve mixed phases. In addition to the complete deconvolution of the ν_{22} mode, new splittings are observed for many other modes. Furthermore, a new lattice mode was observed. Due to use of an edge filter of our Raman spectrometer, low frequency modes below 120 cm^{-1} cannot be recorded from the spectrum. Thus the observation of this mode could be due to either the pressure induced blue shift of a mode below 120 cm^{-1} or a new lattice mode as a result of the formation of a new phase. Most significantly, all the Raman modes exhibit a distinct break in their pressure dependences at this pressure. Therefore, all these observations warrant a phase transition with significantly different molecular orientations with in the unit cell. The observation of the lattice mode indicates that the ordered crystal phase is stable up to 9.5 GPa. In Diky's low-

temperature IR study, two additional solid phases are observed when temperature is lowered below 220 K.[17] The phase observed at 217 K has a dramatically different IR pattern than that above 220 K in that the two strong bands at 480 and 556 cm^{-1} observed at 220 K completely disappeared at 217 K. Since we did not observe any significant change of Raman patterns at either 2.4 or 4.8 GPa, the new phases formed at low temperatures (<220 K) likely are different from those observed around 2.4 and 4.8 GPa and room temperature.

The phase above 10.1 GPa is characterized with broad or convoluted profiles for all Raman modes. Together with the disappearance of the lattice modes, the phase can be interpreted as undergoing a gradual transition to a disordered structure or amorphous phase. Similar features have been observed in 1,2-dichloroethane when pressure is elevated above 9 GPa.[6] Although pressure gradient as a result of nonhydrostatic condition may contribute to the profile broadening, the sudden increase in the bandwidth of several modes (e.g., ν_{47} and ν_{25}) from 9.5 to 10.1 GPa signifies the phase transition. Beyond 10.1 GPa, the profile broadening may be associated with the combination of structural disordering and increasing pressure gradient. At the highest pressure of the present study, the Raman band maintained a similar profile with dominant characteristic Raman modes of ν_{25} and ν_{22}, indicating the six-member ring although highly distorted, still maintains its molecular identity.

The distinctive pressure dependence of all Raman active modes in different pressure regions provides further evidence of phase transitions discussed above. Although the crystal structures of CCH and thus the equation of states characterized by bulk moduli are still unknown, the pressure dependence of most of the Raman modes provides insight on the compressibilities of CCH in different phases. From Fig. 5 and Table II, the majority of the Raman modes exhibit the largest $d\nu/dP$ values below 2 GPa (and especially for the phase between 0.7 and 2 GPa), while those above 5 GPa become significantly smaller, especially beyond 10 GPa. These observations indicate that CCH is more compressible at low pressures less than 2 GPa but relatively less compressible above 10 GPa. The greater compressibility at lower pressure regions is consistent with the general understanding that intermolecular distances are more sensitive to compression and thus make a major contribution to the reduction of the volume.[23]

The most interesting observation is the partial reversibility upon decompression. The decompression measurements reveal a large pressure hysteresis in the high-pressure region above 10 GPa as characterized by the much broader spectral profile upon decompression than compression. Between 10.4 and 2.5 GPa, two new peaks (595 and 711 cm^{-1} at 10.4 GPa or 573 and 697 cm^{-1} at 2.5 GPa) are observed in all the decompression spectra, indicating that the phases formed in this pressure region by decompression are different than those produced by compression. Careful examination of these two new peaks indicates that the frequencies are close to the characteristic ν_{23} and ν_{22} modes of axial conformer. Although other modes associated with axial conformer were not observed, it is plausible to conclude that the phases in this pressure region formed by decompression have the CCH molecules adopting both equatorial and axial conformation. The relative intensity of these two new modes in this pressure region is much smaller than in the liquid phase, indicating that the relative abundance of axial conformation is small. When pressure is further released, the transformation to the first solid phase as well as to the liquid phase is completely reversible as evidenced by almost identical Raman patterns regardless via compression or decompression. The decompression experiment further established that the ring of the CCH sustained compression up to 20 GPa.

It is intriguing that the high-pressure region exhibits hysteresis and partial reversibility. Similar phenomenon was also observed in the low pressure region by Klaeboe.[9] CCH was found to form a polycrystalline phase at about 4 GPa. By carefully releasing pressure followed by gradual compression, a single crystal can be easily grown. On the other hand, considerable "superpressing" results in the spontaneous formation of polycrystalline phase which can be released to 2–2.5 GPa without forming single crystals. All these observations indicate the formation of different phases of CCH is highly *P-T* path dependent. It has also been reported that several organic solids can form the so-called plastic crystals which are characterized with high plasticity in contrast to "normal" organic crystals, which have hard lattice structures and sharp phase transition boundaries.[24] For example, the unsubstituted cyclohexane is a well known plastic crystal at −87 °C and melts at 6 °C.[25] Therefore, the observed pressure-hysteresis and partial reversibility between compression and decompression may be associated with the intrinsic nature of the plasticity of CCH. As plastic crystals have many applications, further detailed structural characterization of CCH at high pressures and different temperatures using more direct probes, such as x-ray diffraction, would be of fundamental interest.

V. CONCLUSIONS

We conducted *in situ* Raman measurements on CCH at room temperature and high pressures up to 20 GPa on both compression and decompression. Below 0.7 GPa, CCH exists as a fluid phase with a mixture of axial and equatorial conformations in equilibrium, which is shifted to axial upon compression. The shift was attributed to the smaller volume of axial conformer with a volume difference of −2.2 $cm^3\ mol^{-1}$ compared to equatorial conformation, consistent with previous studies. When pressure is increased to 2.4 GPa, splittings of the ν_{22} mode as well as the depletion of C–H stretching mode at high frequency indicate a phase transition. The splittings are further enhanced at 4.8 GPa together with the observation of a new lattice mode, suggesting another phase transition. These phases are compared with previously observed phases at low temperatures, which indicates that high-pressure phases are likely different from the low-temperature phases. Compression beyond 9.5 GPa results in significant broadening of Raman profiles, indicating that CCH is undergoing gradual disordering at high pressures. The six-member ring is found to sustain high pressures up to 20 GPa and CCH is fully recoverable upon releasing of

pressure. However, the observation of two new modes upon decompression indicates that phase transformation of CCH is partially irreversible at high pressures above 2.5 GPa. The phase formed by decompression is found to have a contribution from axial conformation of CCH. The partial irreversibility or pressure induced hysteresis is attributed to the plastic nature of the CCH crystals.

ACKNOWLEDGMENTS

The authors are grateful to M. J. Walzak at Surface Science Western for her assistance with the Raman instrumentation. Y.S. and Y.H. acknowledge the supports from Discovery Grants from Natural Science and Engineering Research Council of Canada. Y.S. thanks the Academic Development Fund from the University of Western Ontario.

[1] R. J. Hemley, Annu. Rev. Phys. Chem. **51**, 763 (2000).
[2] R. J. Hemley and H. K. Mao, *Proceedings of the International School of Physics Enrico Fermi*, edited by R. J. Hemley, G. L. Chiarotti, M. Bernasconi, and L. Ulivi (IOS, Amsterdam, 2002), Vol. 147, p. 3.
[3] M. R. Manaa, *Chemistry at Extreme Conditions* (Elsevier, Amsterdam, 2005).
[4] X.-J. Chen, V. V. Struzhkin, Y. Song, A. F. Goncharov, M. Ahart, Z. X. Liu, H. K. Mao, and R. J. Hemley, Proc. Natl. Acad. Sci. U.S.A. **105**, 20 (2008).
[5] Y. Song, Z. X. Liu, H. K. Mao, R. J. Hemley, and D. R. Herschbach, J. Chem. Phys. **122**, 174511 (2005).
[6] R. J. Sabharwal, Y. Huang, and Y. Song, J. Phys. Chem. B **111**, 7267 (2007).
[7] G. Gill, D. M. Pawar, and E. A. Noe, J. Org. Chem. **70**, 10726 (2005).
[8] P. Klaeboe, J. J. Lothe, and K. Lunde, Acta Chem. Scand. (1947-1973) **10**, 1465 (1956).
[9] P. Klaeboe, Acta Chem. Scand. (1947-1973) **23**, 2641 (1969).
[10] T. Woldbaek, Acta Chem. Scand., Ser. A **36**, 641 (1982).
[11] D. J. Gardiner, C. J. Littleton, and N. A. Walker, J. Raman Spectrosc. **18**, 9 (1987).
[12] P. Klaeboe, J. Mol. Struct. **408**, 81 (1997).
[13] S. D. Christian, J. Grundnes, and P. Klaboe, J. Am. Chem. Soc. **97**, 3864 (1975).
[14] G. Waliszewska and H. Abramczyk, J. Mol. Liq. **64**, 73 (1995).
[15] O. Hassel and A. M. Sommerfeldt, Z. Phys. Chem. Abt. B **B40**, 391 (1938).
[16] K. Leibler and J. Przedmojski, J. Chim. Phys. Phys.-Chim. Biol. **59**, 1084 (1962).
[17] V. V. Diky, G. J. Kabo, A. A. Kozyro, A. P. Krasulin, and V. M. Sevruk, J. Chem. Thermodyn. **26**, 1001 (1994).
[18] L. Ciabini, M. Santoro, R. Bini, and V. Schettino, Phys. Rev. Lett. **88**, 085505 (2002).
[19] L. Ciabini, M. Santoro, F. A. Gorelli, R. Bini, V. Schettino, and S. Raugei, Nat. Mater. **6**, 39 (2007).
[20] M. Ceppatelli, M. Santoro, R. Bini, and V. Schettino, J. Chem. Phys. **118**, 1499 (2003).
[21] H. K. Mao, J. Xu, and P. M. Bell, J. Geophys. Res. **91**, 4673 (1986).
[22] D. J. Gardiner and N. A. Walker, J. Mol. Struct. **161**, 55 (1987).
[23] J. R. Ferraro, *Vibrational Spectroscopy at High External Pressures: The Diamond Anvil Cell* (Academic Press, Orlando, 1984).
[24] J. Timmermans, J. Phys. Chem. Solids **18**, 1 (1961).
[25] D. R. MacFarlane and M. Forsyth, Adv. Mater. (Weinheim, Ger.) **13**, 957 (2001).